Braz J Phys (2017) 47:628–639
DOI 10.1007/s13538-017-0525-9

NUCLEAR PHYSICS

A Study of Multi-Λ Hypernuclei Within Spherical Relativistic Mean-Field Approach

Asloob A. Rather[1] · M. Ikram[1] · A. A. Usmani[1] · B. Kumar[2,3] · S. K. Patra[2,3]

Received: 15 June 2017 / Published online: 1 September 2017

Abstract This research article is a follow up of an earlier work by M. Ikram et al., reported in Int. J. Mod. Phys. E **25**, 1650103 (2016) where we searched for Λ magic numbers in experimentally confirmed doubly magic nucleonic cores in light to heavy mass region (i.e., $^{16}O - ^{208}Pb$) by injecting Λ's into them. In the present manuscript, working within the state of the art relativistic mean field theory with the inclusion of ΛN and $\Lambda\Lambda$ interaction in addition to nucleon-meson NL3* effective force, we extend the search of lambda magic numbers in multi-Λ hypernuclei using the predicted doubly magic nucleonic cores $^{292}120$, $^{304}120$, $^{360}132$, $^{370}132$, $^{336}138$, $^{396}138$ of the elusive superheavy mass regime. In analogy to well established signatures of magicity in conventional nuclear theory, the prediction of hypernuclear magicities is made on the basis of one-, two-Λ separation energy (S_Λ, $S_{2\Lambda}$) and two lambda shell gaps ($\delta_{2\Lambda}$) in multi-Λ hypernuclei. The calculations suggest that the Λ numbers 92, 106, 126, 138, 184, 198, 240, and 258 might be the Λ shell closures after introducing the Λ's in the elusive superheavy nucleonic cores. The appearance of new lambda shell closures apart from the nucleonic ones predicted by various relativistic and non-relativistic theoretical investigations can be attributed to the relatively weak strength of the spin-orbit coupling in hypernuclei compared to normal nuclei. Further, the predictions made in multi-Λ hypernuclei under study resembles closely the magic numbers in conventional nuclear theory suggested by various relativistic and non-relativistic theoretical models. Moreover, in support of the Λ shell closure, the investigation of Λ pairing energy and effective Λ pairing gap has been made. We noticed a very close agreement of the predicted Λ shell closures with the survey made on the pretext of S_Λ, $S_{2\Lambda}$, and $\delta_{2\Lambda}$ except for the appearance of magic numbers corresponding to $\Lambda = 156$ which manifest in Λ effective pairing gap and pairing energy. Also, the lambda single-particle spectrum is analyzed to mark the energy shell gap for further strengthening the predictions made on the basis of separation energies and shell gaps. Lambda and nucleon spin-orbit interactions are analyzed to confirm the reduction in magnitude of Λ spin-orbit interaction compared to the nucleonic case, however the interaction profile is similar in both the cases. Lambda and nucleon density distributions have been investigated to reveal the impurity effect of Λ hyperons which make the depression of central density of the core of superheavy doubly magic nuclei. Lambda skin structure is also seen.

Keywords Hypernuclei · Magic number · Separation energy · Spin-orbit interaction · Relativistic mean field theory

1 Introduction

Hypernuclear physics has become an exciting area of research due to the epoch-making strides in the experimental arena. The primary goal of strangeness nuclear physics is to understand the baryon-baryon interaction which is

✉ M. Ikram
ikram@iopb.res.in; ikramamu@gmail.com

1 Department of Physics, Aligarh Muslim University, Aligarh 202002, India

2 Institute of Physics, Bhubaneswar 751 005, India

3 Homi Bhabha National Institute, Anushakti Nagar, Mumbai 400094, India

fundamental and is very important for nuclear physics studies. Two-body scattering is quite useful for elucidating the nature of baryon-baryon interactions. Pursuing this line of thought, many nucleon-nucleon (NN) scattering experiments have been performed. The total number of experiments exceeds 4000. However, because of the difficulty encountered in carrying out the hyperon-nucleon (YN) and hyperon-hyperon (YY) scattering experiments, the YN data available is very scarce. To be more precise, the number of differential cross-section sets of data is nearly about 40 and there is no YY scattering data. Further, the YN and YY potential models put forth so far have large ambiguities in their predictions. Thus, it is imperative and wise to study the structure of single-Λ, double-Λ, and multi-Λ hypernuclei rather than constraining the various theoretical models employing YN and YY potentials. As the number of data points in the hyperon-nucleon sector is small, it is quite difficult to extract the information regarding scattering lengths. This necessitated to analyze this small data using symmetry of $SU(3)_f$ models of baryon-baryon interaction which establishes a close connections with these data in NN sector. However, realistic models must include the symmetry breaking terms as it is badly broken owing to the difference in mass between s and (u,d) quark. Keeping in view the above consideration, various YN potential models have been developed along these lines for hypernuclear studies. The well known models are the Nijmegen models including the hard core models D [1] and F [2], the soft core models NSC89 [3], NSC97 [4], and the extension of soft core models like ESC04 [5], ESC08 [6] which consider two-meson exchanges and other short range contributions in addition to one-boson exchange. In particular, these models enable the extension to hyperon-hyperon potentials, where there is no scattering data available [7], thus implying an unfortunate increase in model dependence. The other type of models known by Bonn-Julich multi-meson exchange models [8–10] which are based on SU(6) symmetry of quark-model. However, the short range nature of YN interaction in these models and Nijmegen models are governed by the way scalar meson interactions are introduced and thus imperactively has got model dependence. The Effective theory chiral model of Leading Order LO [11] and Next Leading Order NLO [12] are another class of model used for hypernuclear studies that makes use of regularized PS Goldstone-boson exchange YN potentials and adding zero-range contact terms for the parameterization of YN coupled-channel interactions and details are reported in Ref. [13]. Further, a quark-model baryon-baryon potential which respects SU(6) symmetry [14] can be used for the construction of hyperon-nucleus potentials [15].

In nuclear physics, the nuclei with magic numbers have been a hot topic since the birth of this subject [16, 17]. With the advent of state of the art radioactive nuclear ion beam (RNIBs) facilities, the quenching of traditional magic numbers and the appearance of new magic numbers have been observed in nuclei with exotic isospin ratios. The explanation of the unusual stability attributed to nuclei with neutron(proton) numbers: 2, 8, 20, 28, 50, 82, and 126 commonly referred to as magic numbers in literature, was given in non-relativistic shell model with a 3D harmonic oscillator central potential in conjunction with a very strong spin orbit interaction added manually [16–20]. Contrary to this, in models which come under the aegis of a relativistic framework, say the relativistic mean-field (RMF) [21–25], the strong spin-orbit interaction is a natural outcome of the interplay between strong scalar and vector potentials, which are indispensable for reproducing the saturation properties of matter. The shell structure is obtained due to proper setting of scalar and vector potentials without incorporating any additional parameter for spin-orbit splitting. The precise location of shell and subshell closures in the nuclear landscape has provided significant inputs needed for the development of nuclear structure models and theories. However, the positions of the shell closures are not static, particularly for exotic nuclei where there are large numbers of neutrons relative to protons. The ongoing experimental endeavors are striving for the location of these shell closures in previously unknown nuclei and trace the movement of the single-particle orbitals which are responsible for this dynamic shell structure. However, we are lucky enough to have a number of experimental observables that show variation at shell closures across the nuclear chart. The nucleon magicity can be inferred from the discontinuity in these observables like separation energy (one- and two-neutron separation energies), two nucleon shell gap, the energies of α and β transitions (nuclear ground-state moments), shell correction energy, pairing correction, effective pairing gap, binding energy, and excitation energy of low-lying vibrational states. Further, nuclear quadrupole moment provides a measure of nuclear charge distribution and hence the nuclear shape. The ground-state quadrupole moment goes to zero at the shell closures and thus the shape of nuclei is expected to be spherical; however, far away from shell closures, the nuclei may be axially deformed and might possess large quadrupole moment. The early theoretical investigation employing macro-microscopic approach predicted the spherically doubly magic nucleus $^{298}114$. However, the existing analysis of magicity using different models showed volatility (variation) in the prediction of shell closures and many reports of investigation were successful in establishing the fact that nuclear magicity is dependent on both model and effective force employed. The inference that can be drawn from these studies that reliability of different parameterizations of the models and the accuracy with which the single-particle energies are estimated plays an indispensable role in heavy and superheavy nuclei owing to the large level density in such nuclei. Thus, it can be concluded that magic numbers in nuclear landscape are fragile/localized and search-space dependent implying that different search space would possibly result in the emergence of different magic numbers.

There is a wealth of literature available regarding the theoretical attempts being made for identifying the nuclear magic numbers in the superheavy region. Some are as follows: within the parameterization of nucleonic mean field in the form of Woods-Saxon potential, Brack et al. [26] explored the nuclear magicity in a wide region of the nuclear chart and suggested the proton magicity at $Z = 114$, 120 and neutron magicity at $N = 184$. In the same vein, the proton magic number at $Z = 114$ and neutron magic number at $N = 184$ were confirmed in the works of refs. [27–30]. The microscopic self-consistent calculations in Hartree-Fock-Bogoliubov (HFB) with effective Gogny forces yielded proton magic numbers at $Z = 114$, 120, and 126 and $N = 164$, 184, and 228 [31]. The parameterizations SLy4 and SkP resulted in the proton magicity at $Z = 124$ and 126 while SkO predicted at $Z = 126$ [32–34]. Further, all these parameterization driven calculations predicted neutron magic number at $N = 184$ [32–35]. Liran et al. [36, 37] predicted proton magicity at $Z = 126$ and neutron magicity at $N = 184$ within the semi-empirical shell model. Calculations within the relativistic HFB approach with finite range pairing force of Gogny effective interaction D_1 and effective interaction NLSH [38] established that $Z = 114$, and $N = 160$, 166, 184 combinations exhibit high stability compared to their neighbors and further doubly magic character at $Z = 106$ and $N = 160$ was predicted in ref. [38]. The non-relativistic Skyrme Hartree Fock (SHF) with effective forces SkP and SLy7 predicted the nuclear magic number at $Z = 126$ and $N = 184$ and in addition presented the evidence of increased stability around $N = 162$ owing to the deformed shell effects [39]. K. Rutz et al. [40] made a prediction about the doubly magic character of $^{298}114$, $^{292}120$, and $^{310}126$. Several other theoretical attempts employing relativistic mean-field models [32, 33, 41, 42] yielded the magic numbers at $Z = 120$ and $N = 172$, 184 while the relativistic model in ref. [43] predicted the nuclear magicity at $Z = 114$, 120 and $N = 172$, 184, and 258 and the reconfirmation of closed shells at $Z = 120$ and $N = 172$, 184, 258 are given in ref. [44]. The exhaustive investigations performed within the framework of continuum relativistic Bogoliubov theory [45] using various effective forces predicted proton numbers $Z = 106$, 114, 120, 126, 132, and 138 and neutron numbers $N = 138$, 164, 172, 184, 198, 216, 228, 238, 252, 258, and 274 as possible magic numbers. The survey made by Denisov on the basis of shell correction calculations [30] predicted spherical proton magic numbers at $Z = 82$, 114, 164, 210, 274, 354 and spherical neutron magic numbers at $N = 126$, 184, 228, 308, 406, 524, 644, 772. Moreover, an extensive study by Nakada and Sugiura [46, 47] over a wide range of even-even nuclei within spherical relativistic mean field approaches with semi-realistic interactions (M3Y-P6 and P7 parameter sets)has been made and they choose the proton(neutron) pairing energy correction and suggested the possible magicity features in the region $Z = 14$, 16, 34, 38, 40, 58, 46, 92, 120, 124, 126 and $N = 40$, 56, 90, 124, 172, 178, 164 and 184, which show remarkable agreements with the results in refs. [48, 49] where Gogny DIS and DIM interactions were used respectively. Further, Ismail et al. [50] have also made more exhaustive investigation regarding the search of nucleonic closed shell within ultra heavy region and predicted a huge number of magic candidates. These predictions have been made on the basis of separation energy, shell gaps, pairing energy and shell correction energy, etc. It has to be mentioned that in a previous work [51] we have inferred lambda magicity is in quite close agreement with nucleon magicity which arouse us to investigate lambda magic number in more exotic region and its predictions would give strong evidence about the confirmation of nuclear magicity in superheavy regime. The work in the present manuscript is also supposed to be another attempt in support of nuclear magicity of superheavy region. Among the different methodologies used for identifying the nuclear magicity, we adopt the calculations of one-, two- Λ separation energies, two Λ shell gaps, lambda pairing energy, and effective lambda pairing gap to study lambda magicity for the considered set of multi-Λ hypernuclei. Thus, in this paper, our main emphasis would be to make extensive investigation to search the Λ magic number in multi-Λ hypernuclei within the spherical relativistic mean field approach as well as to suggest the confirmation of nucleon magic number of superheavy region within the favour of Λ magicity. The subject matter of manuscript is organized as follows: the theoretical framework of spherical relativistic mean field model is outlined in Section 2. Section 3 contains the results and discussion. Finally, the paper is summarized in Section 4.

2 Theoretical Formalism

Relativistic mean field theory has established itself as a promising theoretical framework to study the infinite nuclear systems, finite nuclei including the superheavy mass region, hypernuclei, and multi-strange systems [52–59]. The suitable extension to strangeness sector for studying the hypernuclei and multi-Λ hypernuclei is accomplished by incorporating the lambda-baryon as well as lambda-lambda interactions Lagrangian with effective ΛN and $\Lambda\Lambda$ potentials in addition to nucleon-meson NL3* force parameter and such type of attempts have already been made [52–59]. For quantitative description of the multi-Λ hypernuclei, additional strange scalar (σ^*) and vector (ϕ) mesons have been incorporated in the the Lagrangian which simulate the $\Lambda\Lambda$ interaction [60–63]. Thus, the total Lagrangian density can be expressed as follows:

$$\mathcal{L} = \mathcal{L}_N + \mathcal{L}_\Lambda + \mathcal{L}_{\Lambda\Lambda}, \quad (1)$$

$$\begin{aligned}\mathcal{L}_N =& \bar{\psi}_i\{i\gamma^\mu\partial_\mu - M\}\psi_i + \frac{1}{2}(\partial^\mu\sigma\partial_\mu\sigma - m_\sigma^2\sigma^2) - \frac{1}{3}g_2\sigma^3 \\ &-\frac{1}{4}g_3\sigma^4 - g_s\bar{\psi}_i\psi_i\sigma - \frac{1}{4}\Omega^{\mu\nu}\Omega_{\mu\nu} + \frac{1}{2}m_\omega^2\omega^\mu\omega_\mu \\ &-g_\omega\bar{\psi}_i\gamma^\mu\psi_i\omega_\mu - \frac{1}{4}B^{\mu\nu}B_{\mu\nu} + \frac{1}{2}m_\rho^2\vec{\rho}^\mu\vec{\rho}_\mu - \frac{1}{4}F^{\mu\nu}F_{\mu\nu} \\ &-g_\rho\bar{\psi}_i\gamma^\mu\vec{\tau}\psi_i\vec{\rho^\mu} - e\bar{\psi}_i\gamma^\mu\frac{(1-\tau_{3i})}{2}\psi_i A_\mu\,, \end{aligned}\quad (2)$$

$$\mathcal{L}_\Lambda = \bar{\psi}_\Lambda\{i\gamma^\mu\partial_\mu - m_\Lambda\}\psi_\Lambda - g_{\sigma\Lambda}\bar{\psi}_\Lambda\psi_\Lambda\sigma - g_{\omega\Lambda}\bar{\psi}_\Lambda\gamma^\mu\psi_\Lambda\omega_\mu \quad (3)$$

$$\begin{aligned}\mathcal{L}_{\Lambda\Lambda} =& \frac{1}{2}(\partial^\mu\sigma^*\partial_\mu\sigma^* - m_{\sigma^*}^2\sigma^{*2}) - \frac{1}{4}S^{\mu\nu}S_{\mu\nu} + \frac{1}{2}m_\phi^2\phi^\mu\phi_\mu \\ &-g_{\sigma^*\Lambda}\bar{\psi}_\Lambda\psi_\Lambda\sigma^* - g_{\phi\Lambda}\bar{\psi}_\Lambda\gamma^\mu\psi_\Lambda\phi_\mu\,, \end{aligned}\quad (4)$$

where ψ and ψ_Λ denote the Dirac spinors for nucleon and Λ hyperon, whose masses are M and m_Λ, respectively. Due to the isoscalar nature of Λ hyperon, it does not couple to ρ-mesons. The quantities m_σ, m_ω, m_ρ, m_{σ^*}, m_ϕ represent the masses of σ, ω, ρ, σ^*, ϕ mesons and g_s, g_ω, g_ρ, $g_{\sigma\Lambda}$, $g_{\omega\Lambda}$, $g_{\sigma^*\Lambda}$, $g_{\phi\Lambda}$ are their coupling constants, respectively. The nonlinear self-coupling of σ-mesons is designated by by g_2 and g_3. The total energy of the system is given by $E_{total} = E_{part}(N,\Lambda) + E_\sigma + E_\omega + E_\rho + E_{\sigma^*} + E_\phi + E_c + E_{pair} + E_{c.m.}$, where $E_{part}(N,\Lambda)$ is the sum of the single-particle energies of the nucleons (N) and hyperons (Λ). The energies parts E_σ, E_ω, E_ρ, E_{σ^*}, E_ϕ, E_c, E_{pair}, and E_{cm} are the contributions of meson fields, Coulomb field, pairing energy, and the center of mass energy, respectively. There is wealth of available literature about RMF parameterizations for predicting the nuclear ground state properties. In the present manuscript, NL3* parameterization is employed for meson-baryon coupling constant throughout the calculations [64]. To find the numerical values of used $\Lambda-$meson coupling constants, we adopt the nucleon coupling to hyperon couplings ratio defined as follows: $R_\sigma = g_{\sigma\Lambda}/g_\sigma$, $R_\omega = g_{\omega\Lambda}/g_\omega$, $R_{\sigma^*} = g_{\sigma^*\Lambda}/g_\sigma$, and $R_\phi = g_{\phi\Lambda}/g_\omega$. The relative coupling values are used as $R_\omega = 2/3$, $R_\sigma = 0.6104$, $R_\phi = -\sqrt{2}/3$, and $R_{\sigma^*} = 0.69$ [62, 65, 66]. The coupling constants of hyperons to vector mesons have to be compatible with the maximum neutron star masses and are fitted to the Λ binding energy in nuclear matter [67]. The predictions of maximum neutron star mass using NL3* parameterization is reported recently in ref. [68]. The maximum neutron star mass using NL3* without the inclusion of hyperons comes out to be 2.81 $M_\odot$ and is thus overestimating the recently measured experimental values [69, 70]. In particular, with the inclusion of hyperons in equation of state, the maximum neutron star mass comes out to be 1.91 $M_\odot$ which is in close agreement with experimental data [69, 70]. The used NL3* parameter set and their nuclear matter properties around saturation point are listed in Table 1 which are taken from ref. [71].

Table 1 The used NL3* parameter set and their nuclear matter saturation properties are hereby given [71, 72]

Parameters of NL3*	
M = 939 MeV	
m_σ = 502.5742 MeV	g_σ = 10.0944
m_ω = 782.6 MeV	g_ω = 12.8065
m_ρ = 763.0 MeV	g_ρ = 4.5748
g_2 = −10.8093 fm^{-1}	g_3 = −30.1486
Nuclear matter properties	
ρ_0 = 0.150 fm^{-3}	(Saturation density)
$(E/A)_\infty$ = 16.31 MeV	(Infinite nuclear matter binding energy)
m*/m = 0.594	(Ratio of effective mass and bare mass)
K_0 = 258.27 MeV	(Incompressibility)
J = S(ρ_0) = 38.68 MeV	(Symmetry energy)
L_0 = 122.63 MeV	(Slope of S)
$K^0_{symmetry}$ = 105.56 MeV	(Curvature of S)

These mentioned nuclear matter properties are in close agreement with the giant dipole resonance (GDR) and giant monopole resonance (GMR) experimental energies [72]. In present calculations, we use the constant gap BCS approximation to include the pairing interaction and the centre of mass correction is included by $E_{cm} = -(3/4)41A^{-1/3}$.

3 Results and Discussions

In the present manuscript, we made an attempt to look for the magic candidates in multi-Λ hypernuclei under investigation on the basis of one-, two-Λ separation energies, two lambda shell gaps and pairing energy/gaps, etc. by performing calculations within the self-consistent relativistic mean-field model using NL3* parameterization with inclusion of ΛN and $\Lambda\Lambda$ interactions. Our quest of hunt for magic numbers in multi-Λ hypernuclei with doubly magic superheavy nucleonic cores receives the motivation from the seminal work of Zhang et al. [45] wherein they made an extensive investigation by performing calculations within relativistic continuum Hartree-Bogoliubov theory and established that $Z = 120$, 132, 138 and $N = 172$, 184, 198, 228, 238, and 258 might be the possible nucleonic magic numbers. Further, Ismail et al. [50] have made more exhaustive investigation about the search of nucleonic shell closures and predicted a huge number of magic candidates in ultra heavy region. We extend this line of thought toward strangeness sector with more exotic lambda region and try to predict a triple magic

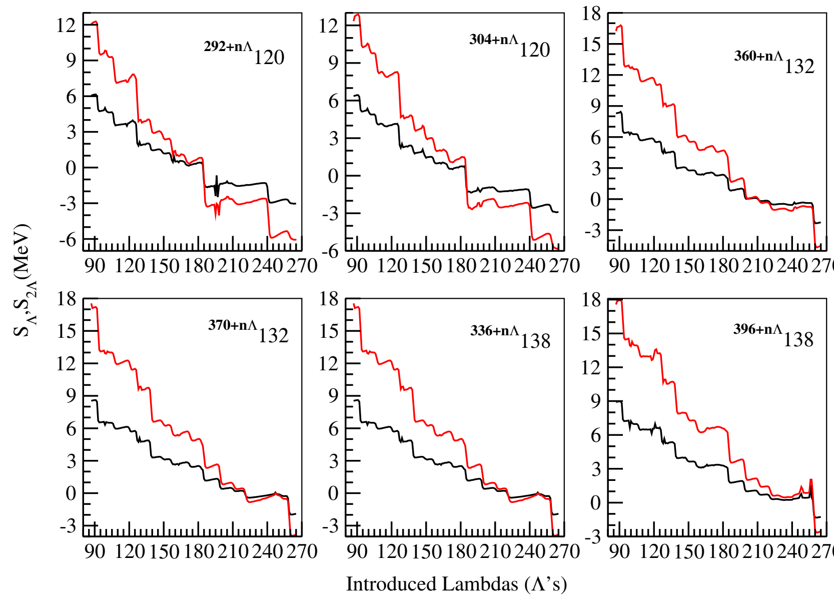

Fig. 1 One- and two-Λ separation energy for multi-Λ hypernuclei as a function of introduced Λ's. Black lines represent the S_{Λ} while $S_{2\Lambda}$ is shown by red lines (color online)

multi-Λ system having doubly magic superheavy nucleonic core.

3.1 Lambda Separation Energy and Two Lambda Shell Gaps

The separation energy is an important physical quantity and is of paramount importance for locating and identifying the magic numbers in nuclei as well as hypernuclei. The magic character is manifested by the presence of large shell gaps in the single-particle spectrum of nuclei(hypernuclei). This in turn implies that the nucleons (hyperons) in the lower energy levels has got more binding energy than the nucleons(hyperons) in upper energy levels. The reliable measures of one- and two-nucleon separation energies for marking the shell closures in conventional nuclear theory can be conveniently carried out to strangeness sector and may be expressed as follows.

$$S_{\Lambda}(N, Z, \Lambda) = BE(N, Z, \Lambda) - BE(N, Z, \Lambda - 1) \quad (5)$$

and,

$$S_{2\Lambda}(N, Z, \Lambda) = BE(N, Z, \Lambda) - BE(N, Z, \Lambda - 2) \quad (6)$$

These quantities are plotted in Fig. 1. Moreover, two-Λ separation energy is more efficient marker of magic numbers than one-Λ separation energy due to the absence of odd-even staggering. For the considered lambda chain (Λ = 90–265), the binding energy increases up to a certain limit by increasing the number of injected Λ's in considered doubly magic nucleonic cores. However, for a fixed N, Z combination, the S_{Λ} and $S_{2\Lambda}$ show a gradual decreasing trend with the number of injected Λ's. A sudden fall in S_{Λ} and $S_{2\Lambda}$ in analogy to neutron and proton chains indicates the occurrence of Λ shell closure. The abrupt decrease in the value of $S_{2\Lambda}$ at Λ = 92, 106, 126, 138, 184, 198, 240, 258 can be easily seen in the multi-Λ hypernuclei under investigation thus revealing their magic character. Thus, these numbers correspond to Λ magic numbers in the multi-Λ hypernuclei and form the triply magic system with doubly magic superheavy nucleonic cores. In order to provide a clear presentation of magicity features, the shell effects are also quantified in terms of two lambda shell gaps which is a carry over from the conventional nuclear physics. The two lambda shell gap is expressed as follows:

$$\begin{aligned}\delta_{2\Lambda}(N, Z, \Lambda) &= 2BE(N, Z, \Lambda) - BE(N, Z, \Lambda + 2) \\ &\quad - BE(N, Z, \Lambda - 2) \\ &= S_{2\Lambda}(N, Z, \Lambda) - S_{2\Lambda}(N, Z, \Lambda + 2) \quad (7)\end{aligned}$$

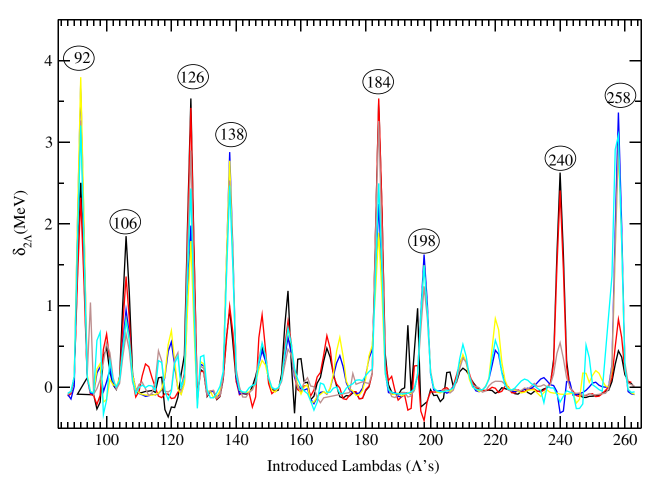

Fig. 2 Two-lambda shell gap for considered superheavy mass multi-Λ hypernuclei as a function of introduced Λ's (color online)

Two lambda shell gap is considered to be strong signature for identifying the magic numbers. Two lambda shell versus number of injected lambdas is plotted in Fig. 2 for all the considered multi-Λ hypernuclei under investigation. A peak in the two lambda shell gap indicates the drastic change in two-Λ separation energies. A peak at certain Λ number hints toward the Λ shell closure. However, the quality of Λ shell gap is dictated by the sharpness and magnitude of the peak. From Fig. 2, the peaks at Λ = 92, 106, 126, 138, 184, 198, 240, and 258 are evident and these numbers are suppose to be Λ magic numbers.

3.2 Lambda Pairing Energies and Pairing Gaps

Pairing is an important ingredient in a mean-field description of nuclear structure calculations [73]. It is worthy to mention that the pairing correlation is significant for open shell nuclei with a large density of almost degenerated states, which offers an opportunity to residual two-body interaction to mix these states in order to produce a unique ground-state [74]. This means the pairing contribution in total energy is very less or almost zero for closed shell nuclei. The two mostly used methods to treat pairing are HFB and BCS approximation. In HFB, pairing correlations are taken into account by introducing the concept of quasi-particles defined by Bogoliubov transformation while as BCS approximation is just a simplification of HFB for time-reversal invariant systems [75]. In both of these schemes, each single nucleon state ϕ_α is associated with an occupation amplitude $v_\alpha \in [0, 1]$ where the complementing non-occupation amplitude is $u_\alpha = \sqrt{1 - v_\alpha^2}$.

This refer to that pairing energy may serve as a reliable source of information for identifying the closed shell nuclei or hypernuclei. In BCS approximation, the Λ pairing energy is defined in terms of effective pairing gap Δ and occupations as given by

$$E_{pair} = -\Delta \sum_\alpha \sqrt{w_\alpha(1 - w_\alpha)}. \tag{8}$$

In order to ensure successful calculation of every desired nucleus, occupation numbers w_α are allowed to vary between 0 and 1, whose values are determined using schematic pairing within the constant gap approach using single-particle energy spectrum [76]

$$w_\alpha = \left(\frac{1}{2} + \frac{\epsilon_\alpha - \epsilon_{Fermi}}{\sqrt{(\epsilon_\alpha - \epsilon_{Fermi})^2 + \Delta^2}} \right)^{1/2} \tag{9}$$

where

$$\Delta = \frac{11.2MeV}{\sqrt{A}} \tag{10}$$

and the Fermi energy is determined by

$$\sum_{\alpha=1}^{\Omega} W_\alpha = \begin{cases} \text{number of protons or} \\ \quad \text{number of neutrons} \end{cases} \tag{11}$$

where Ω is the number of shell model states incorporated for protons, or for neutrons respectively and further, we always include one shell above the last closed shell.

The outcome of Λ pairing energy and effective pairing gaps for considered multi-Λ hypernuclei under investigation are plotted in Fig. 3. Figure 3 reveals the minimum contribution of pairing energy indicating by peaks at lambda number 92, 106, 126, 138, 156, 184, 198, 240, 258 which are suggested to be Λ shell closure in strangeness sector. The suggested magic number on the basis of Λ pairing energy and effective Λ pairing gaps are in close agreement

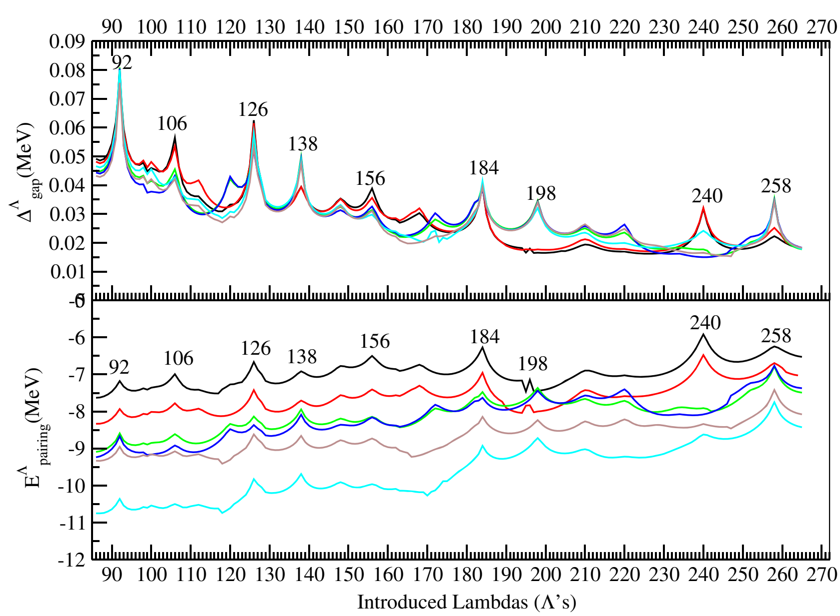

Fig. 3 The effective Λ pairing gap (Δ^{Λ}_{gap}) as a function of Λ number as given in upper panel. The Λ pairing energies ($E^{\Lambda}_{pairing}$) as a function of Λ number shown in lower panel (color online)

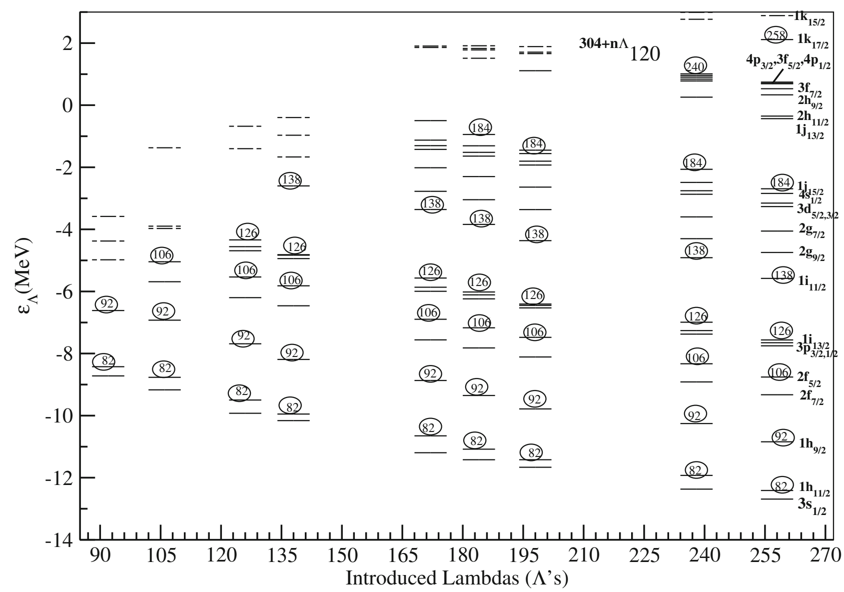

Fig. 4 Lambda single-particle energy levels for $^{304+n\Lambda}120$ multi-Λ hypernuclei for $\Lambda = 92, 106, 126, 138, 172, 184, 198, 240$, and 258. Filled levels are represented by solid lines whereas dashed line represents the unoccupied levels of the given system

with other signatures of magicity discussed earlier in the manuscript except $\Lambda = 156$ which make their appearances in effective Λ pairing gap and pairing energy respectively for the chosen set of multi-Λ hypernuclei.

3.3 Lambda Single-Particle Energy Spectrum

The single-particle spectrum reflects any kind of change occurring in a system either normal nuclei or hypernuclei. In order to analyze the effects of hyperon addition to the predicted doubly magic nucleonic cores and to confirm or provide the support to our calculations, we have plotted the lambda single-particle energy levels $^{304+n\Lambda}120$, $^{360+n\Lambda}132$, and $^{396+n\Lambda}138$ systems as given in Figs. 4, 5 and 6. The prescription for filling the lambda energy levels is quite similar to that of nucleon energy levels filled according to shell model scheme. However, it is evident that the single-particle energy gap between lambda levels is smaller as compared to gaps in nucleon single-particle energy scheme owing to relatively weaker strength of Λ spin-orbit interaction. In previous article [51], we have analyzed the Λ single-particle energy levels up to the filling of 82 lambdas and predicted the Λ magic number from 2 to 82. Therefore, in the present case, we analyze the higher levels above the filling of 82

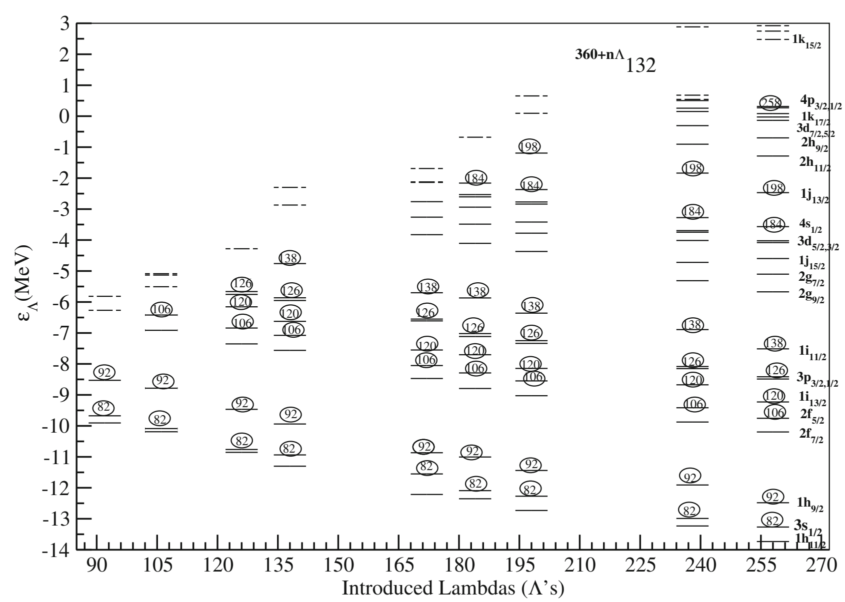

Fig. 5 Same as Fig. 4 but for superheavy mass $^{360+n\Lambda}132$ multi-Λ hypernuclei

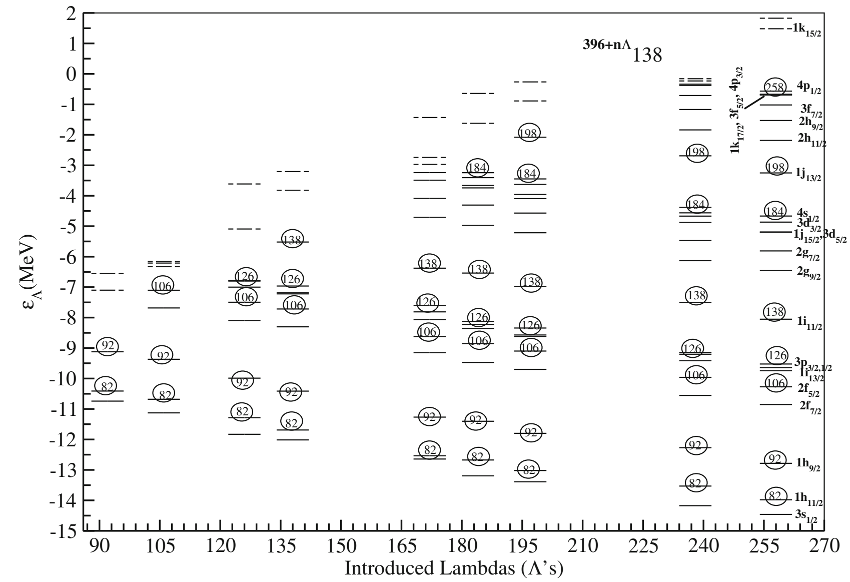

Fig. 6 Same as Fig. 4 but for superheavy mass $^{396+n\Lambda}138$ multi-Λ hypernuclei

Λ's to look for the lambda magicity in higher region. To make this things, we focused on $^{304+n\Lambda}120$, $^{360+n\Lambda}132$, and $^{396+n\Lambda}138$ superheavy multi-Λ hypernuclei.

After carefully analyzing the single-particle energy diagram of $^{360+n\Lambda}$ 132, a large gap exists between 1h9/2 and $2f_{7/2}$ thus resulting in the appearance of $\Lambda = 92$ as strong magic shell closure. This is followed by a relatively smaller gap between $2f_{5/2}$ and $1i_{13/2}$ thus making $\Lambda = 106$ a relatively weak magic number compared to $\Lambda = 92$. Further, the energy gaps between $1i_{13/2}$ and $3p_{1/2}$, $3p_{1/2}$ and $1i_{11/2}$ are large compared to the previous case. This results in the emergence of relatively strong magic numbers at $\Lambda = 120$ and $\Lambda = 126$, respectively. Moreover, the energy gap between $1i_{11/2}$ and $2g_{9/2}$ is of comparable magnitude to the energy gap corresponding to $\Lambda = 92$ magic number and thus makes $\Lambda = 138$ a strong magic number. In addition, two gaps of almost same magnitude between $4s_{1/2}$ to $1j_{13/2}$ and $1j_{13/2}$ to $2h_{11/2}$ which hints toward the two strong magic numbers corresponding to $\Lambda = 184, 198$. Moreover, a large energy gap is observed between $4p_{1/2}$ and $1k_{15/2}$ which results in $\Lambda = 258$ as strong magic number. The identical Λ magic numbers are reproduced in $^{396+n\Lambda}138$ except for $\Lambda = 120$ which disappears or gets quenched. The shell closure at $\Lambda = 120$ is quenched in $^{304+n\Lambda}120$; however, large shell gap between $4p_{1/2}$ to $1k_{17/2}$ is appeared resulting the emergence of $\Lambda = 240$ magic number. Some inversion of lambda levels is noticed in considered multi-hypernuclear candidates. For example, $3s_{1/2}$ filled faster than $1h_{11/2}$ in case of $^{304+n\Lambda}120$, $^{396+n\Lambda}138$ which is inverted in case of $^{360+n\Lambda}132$. The lambda level $4p_{1/2}$is the last filled level in $^{396+n\Lambda}138$ and $^{360+n\Lambda}132$ while this level got inverted with $1k_{17/2}$ in $^{304+n\Lambda}120$. Therefore, a inversion between $\{4p_{1/2}, 1k_{17/2}\}$ and $\{3s_{1/2}, 1h_{11/2}\}$ is observed. The inversion or filling of higher levels faster than lower one and hence this type of filling is responsible for emerging the variation in prediction of new magic number and this is due to the spin-orbit interaction. This is also seen here for example, 120 is appeared to be Λ magic number in some systems which is quenched in others. Also, 240 is appeared only in $^{304+n\Lambda}120$ and $^{292+n\Lambda}120$ but missed in other systems. In general, it is quite worth to mention that pronounced shell gaps for lambda number 92, 106, 126, 138, 184, 198, 240, and 258 are noticed in considered multi-Λ hypernuclei and being suggest to be strong Λ shell closures as well as reflected in $\delta_{2\Lambda}$ calculations.

3.4 Lambda Magicity

The impetus for searching the magic numbers in hypernuclear physics earns its motivation from the ever evolving search of magic numbers in conventional nuclear physics. This encourages us to look for the magicity in strangeness sector. We conducted a study on the multi-Λ hypernuclei under investigation within the powerful framework of spherical relativistic mean field with NL3* nucleon-meson

Table 2 Lambda magic number produced in various considered multi-Λ hypernuclei are tabulated here

Hypernuclei	Lambda magic numbers								
$^{292+n\Lambda}120$	92	106	–	126	138	184	198	240	258
$^{304+n\Lambda}120$	92	106	–	126	138	184	198	240	258
$^{360+n\Lambda}132$	92	106	120	126	138	184	198	–	258
$^{370+n\Lambda}132$	92	106	–	126	138	184	198	–	258
$^{336+n\Lambda}138$	92	106	–	126	138	184	198	–	258
$^{396+n\Lambda}138$	92	106	–	126	138	184	198	–	258

parameterization in inclusion of ΛN as well as ΛΛ interactions. Prediction of magic numbers in superheavy region within various theoretical models is a debated subject which arouse our interest to look for magicity in strangeness sector. After analyzing the S_Λ and $S_{2\Lambda}$ for the multi-Λ hypernuclei, we noticed a sudden fall in separation energy is observed at Λ = 92, 106, 126, 138, 184, 198, 240, and 258 and we conclude that these numbers might be the possible Λ magic numbers in the multi-Λ hypernuclei given in Table 2. In order to make a stringent test to our findings and to confirm our calculations based on S_Λ and $S_{2\Lambda}$, we made investigation on the basis of two lambda shell gap which is considered to be the strong signature of magicity. We observed that the predictions made on the basis of $\delta_{2\Lambda}$ are in tune with the possibilities on the pretext of S_Λ and $S_{2\Lambda}$. A pronounced peak is observed for Λ = 92, 126, 138, 184, 240, and 258 in the two lambda shell gap signaling the presence of strong shell closure. The peak at Λ = 106, 198 are of slightly less magnitude then the others. Moreover, in favor of Λ predictions the investigation of Λ pairing energy and effective Λ pairing gap has been made and its outcome are found to be in very close agreement with the survey made on the pretext of separation energy and shell gaps. Further, in order to support in these calculation and to reveal the magic nature of these numbers, we analyzed the lambda single-particle energy spectrum of $^{304+n\Lambda}120$, $^{360+n\Lambda}132$, and $^{396+n\Lambda}138$. Inspection of the single-particle energies for these chosen multi-Λ hypernuclei reveals a large shell gaps at Λ = 92, 106, 120, 126, 138, 184, 198, 240, and 258. The shell gaps at Λ = 120 does not appear in all investigated candidates and make its appearance only in $^{360+n\Lambda}132$. This leads us to the conclusion that Λ = 120 is not a strong magic number in strangeness physics and might be considered as very feeble magic number, however, it is predicted to be a strong proton magic number supported by many theoretical investigations. The predicted Λ magic number in present calculations quite resembles with the nuclear magic number of superheavy region. Therefore, it can be concluded that Λ magicity resembles quite closely with the predicted magic numbers in enigmatic superheavy valley. The investigations about magic numbers might serve as a significant input to reveal important information regarding new nucleonic shell closures.

3.5 Lambda and Nucleon Spin-Orbit Interaction Potentials

It has already been mentioned that YN data available is very scanty. Moreover, a very little know about the spin-dependent interaction such as spin-orbit force and hence the spin-orbit splitting in ΛN interaction has become a subject of study in strangeness physics. Lambda spin-orbit coupling has been found to be smaller than that of nucleons and no definite value is produced by the experiment [77–80]. The smallness of Λ spin-orbit splitting in ΛN interaction was first suggested in the (K^-, π^-) reaction on ^{16}O [77]. The smaller magnitude of Λ spin-orbit potential is encountered due to the presence of antisymmetric part of spin-orbit force in ΛN interaction, i.e., {l.$(S_\Lambda - S_N)$} and also by the energy difference of single-particle states of j = l − 1/2 and j = l +1/2. These two parts of spin-dependent force tend to cancel in ΛN interaction which leads to a small amount of lambda spin-orbit splitting in Λ single particle states. However, for quantitative description of spin-orbit force, various theoretical relativistic and non-relativistic models with suitable effective force have been employed. In non-relativistic model, the spin-orbit force is included manually while it is naturally developed in relativistic approaches

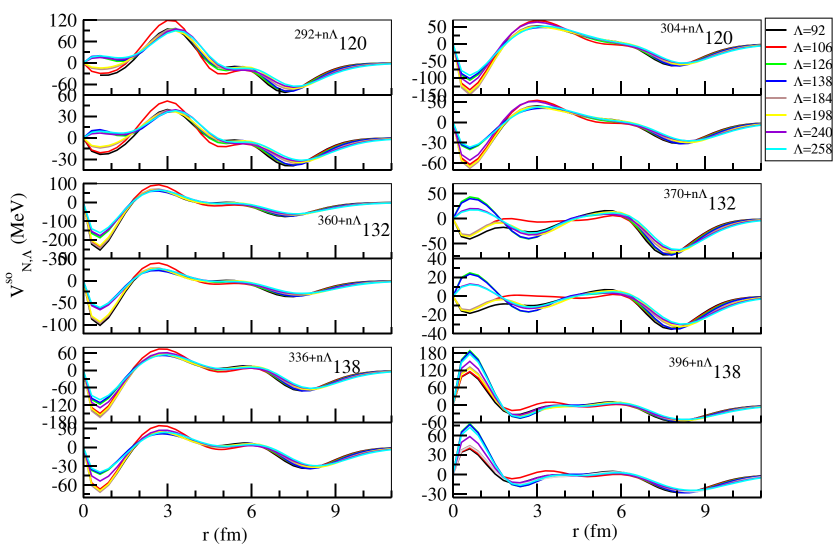

Fig. 7 Spin-orbit interaction potentials of nucleons and Λ hyperons for considered superheavy multi-Λ hypernuclei for lambda number 92, 106, 126, 138, 184, 198, 240, and 258 as function of radial parameter. The upper part in each panel represent the nucleon spin-orbit and the lower one representing the Λ spin-orbit potentials (color online)

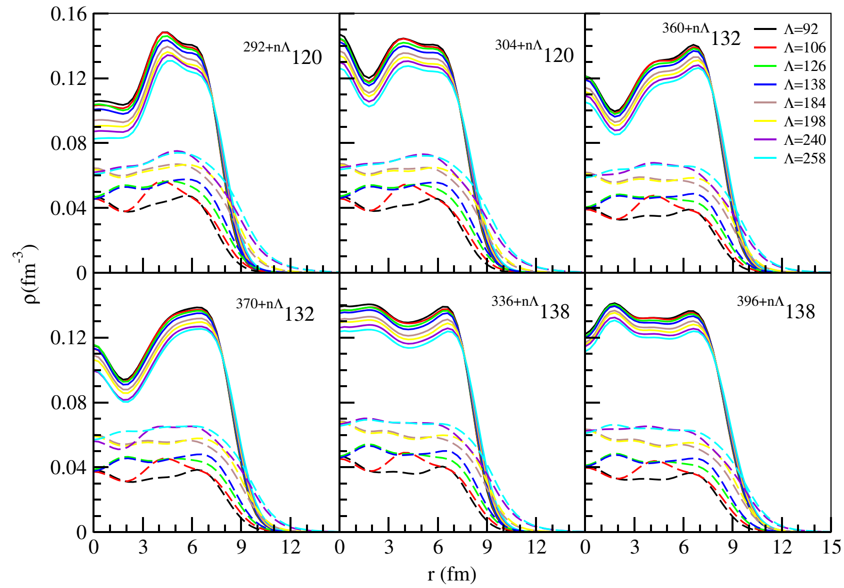

Fig. 8 Nucleon and Λ density profile for considered superheavy multi-Λ hypernuclei for Λ number 92, 106, 126, 138, 184, 198, 240, and 258. Nucleon density is represented by solid lines whereas Λ density by dashed lines (color online)

such as RMF and spin-orbit potential emerges automatically with the empirical strength. This coupling is very crucial for quantitative description of nuclear or hypernuclear structure as well as in order to reproduce the empirical magic numbers. In the present case, we analyzed the nucleon as well as Λ spin-orbit interaction potentials for considered multi-Λ hypernuclei as shown in Fig. 7, where we found a consistency in nucleonic and hyperonic splitting as previous predictions that implies reduction of Λ spin-orbit is about 30–40% of nucleonic case. For example, for $^{292+n\Lambda}$120 at $r = 3$ fm, the V_N^{so} is about of 120 MeV and this value reduced to 45 MeV for V_Λ^{so} that comes out to be around 40% of nucleonic potentials. It is quite evident that both the potentials are different by their depth but have the similar interaction shape. Further inspection reveal that injection of Λ's significantly affects the nucleon as well as Λ spin-orbit potential to a large extent.

3.6 Density Profile

It is worthy to mention that the injected Λ hyperon affects the every piece of physical observables such as size, shape, binding energy, density distribution, etc. Therefore, it is quite interesting as well as important to study the effects of large number of Λ on the nuclear density and hence the distribution of nucleons and Λ hyperons in considered multi-Λ

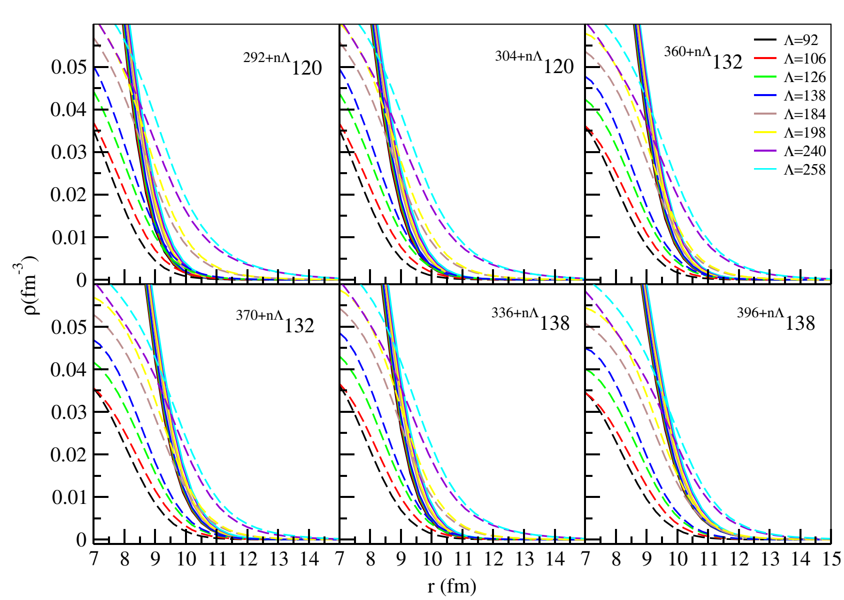

Fig. 9 Same as Fig. 8 but for peripheral region (color online)

systems is analyzed by means of density profile as shown in Fig. 8. From this figure, we noticed that the successive addition of Λ hyperons reduces the magnitude of central nuclear density resulting increases the matter radii of the system. This is happened because injected lambdas are sitting in higher orbitals that attributed to increase the size of the system. For example, in case of $^{292+n\Lambda}120$, the magnitude of central density for $\Lambda = 92$ is 0.11 fm^{-3}, whereas this value reaches to 0.08 fm^{-3} for $\Lambda = 258$ indicating a reduction of central density. In other words, we can say that the excessive addition of Λ hyperons depressed the central region of nuclear core. This implies that the presence of large number of Λ's pushes out the nucleons from the central region. Moreover, only magnitude of central density is reduced while the shape of profile is unaltered. Further inspection reveals that the lambda density increases with successive addition of Λ hyperons and that is obvious. Since, there is no change of nucleon numbers and hence no anomalous behavioo̊f nuclear density is encountered in considered multi-Λ hypernuclei. Moreover, for the sake of skin/halo structure, we analyzed the behavior of lambda and nucleon density profile at peripheral region. For this, we make a plot of density profile at radial parameter $r = 7$ to 15 fm shown in Fig. 9. The nucleon density dies at $r = 11$ fm while Λ density extended to 14 fm as evident in case of $^{292+n\Lambda}120$ and $^{304+n\Lambda}120$ and others also. This dictate that the presence of large number of Λ's pushes the lambda itself toward the periphery of the system and this kind of behavior of Λ distribution form a Λ skin structure.

4 Summary and Conclusions

In the present work, we performed spherical relativistic calculations with ΛN and ΛΛ interactions in multi-Λ hypernuclei and postulated the possible Λ magic numbers, i.e., 92, 106, 120, 126, 138, 184, 198, 240, 258. These predictions have been made by the survey employing various signatures of magicity in strangeness sector like one- and two-Λ separation energy and two lambda shell gaps. We witnessed prominent peaks as well as single-particle energy gaps for lambda numbers 92, 126, 184, and 258. Further, the predictions made in multi-Λ hypernuclei under study resembles quite closely the magic numbers in conventional nuclear theory suggested by various relativistic and non-relativistic theoretical models and these Λ predictions also support the confirmation of nucleon magicity of superheavy regime. Thus, it can be inferred that YN interaction is of similar nature as NN interaction except for its weaker strength compared to the nucleonic case. The appearance of new lambda shell closures apart from the nucleonic ones predicted by various theoretical approaches in superheavy mass regime can be attributed to the relatively weak strength of the spin-orbit interaction in the strange sector. Further, to lend a support to our calculations, we explore the occurrence of spherical shell closures by doing a survey on the basis of lambda pairing energy and effective lambda pairing gap and the results are quite consistent with the predictions made using S_Λ, $S_{2\Lambda}$, and $\delta_{2\Lambda}$ except for the appearance of a magic number at $\Lambda = 156$ which emerges from the lambda effective pairing gap and pairing energy within the considered multi-Λ hypernuclei. Lambda single-particle spectrum is also analyzed to mark the energy shell gap for further strengthening the predictions made on the basis of separation energy and shell gaps. Lambda and nucleon spin-orbit interactions are analyzed to confirm the reduction in magnitude of the Λ spin-orbit interaction to the nucleonic case; however, the interaction profile is similar in both the cases. It is also concluded that the addition of Λ's significantly affects the nucleon as well as the Λ spin-orbit potential. Lambda and nucleon density distributions have been made to further confirm the impurity effect of Λ hyperons which make the reduction in magnitude of central density of the cores. Lambda skin structure is also reported. The stability attributed to the doubly magic superheavy cores by addition of hyperons may serve as a motivation for experimentalists to synthesize these triply magic system in a near future. This might provide significant input and shed some light on novel features of new nucleonic shell closures. Further, superheavy nucleonic cores (doubly magic) are seen to be more likely to absorb large number of hyperons. Hence, it can be said that such systems replicate the strange hadronic matter containing multiple degrees of strangeness (multi-strange) such as Σ's, Ξ's and hyperons which has got huge importance in nuclear astrophysics like neutron stars, hyperon stars, etc.

Acknowledgements One of the authors (MI) would like to acknowledge the hospitality provided by Institute of Physics (IOP), Bhubaneswar where the parts of this work was carried out.

References

1. M.M. Nagels, T.A. Rijken, J.J. de Swart, Phys. Rev. D **15**, 2547 (1977)
2. M.M. Nagels, T.A. Rijken, J.J. de Swart, Phys. Rev. D **20**, 1633 (1979)
3. P.M.M. Maessen, T.A. Rijken, J.J. de Swart, Phys. Rev. C **40**, 2226 (1989)
4. T.A. Rijken, V.J.G. Stoks, Y. Yamamoto, Phys. Rev. C **59**, 21 (1999)
5. T.A. Rijken, Y. Yamamoto, Phys. Rev. C **73**, 044008 (2006)
6. M.M. Nagels, T.A. Rijken, Y. Yamamoto, arXiv:1501.06636 (2015)
7. M.M. Nagels, T.A. Rijken, Y. Yamamoto, arXiv:1504.02634 (2015)
8. B. Holzenkamp, K. Holinde, J. Speth, Nucl. Phys. A **500**, 485 (1989)

9. A. Reuber, K. Holinde, J. Speth, Nucl. Phys. A **570**, 543 (1994)
10. J. Haidenbauer, U.-G. Meißner, Phys. Rev. C **72**, 044005 (2005)
11. H. Polinder, J. Haidenbauer, U.-G. Meißner, Nucl. Phys. A **779**, 244 (2006)
12. J. Haidenbauer, S. Petschauer, N. Kaiser, U.-G. Meißner, A. Nogga, W. Weise, Nucl. Phys. A **915**, 24 (2013)
13. J. Haidenbauer, Nucl. Phys. A **914**, 220 (2013)
14. Y. Fujiwara, Y. Suzuki, C. Nakamoto, Prog. Part. Nucl. Phys. **58**, 439 (2007)
15. M. Kohno, Y. Fujiwara, Phys. Rev. C **79**, 054318 (2009)
16. M.G. Mayer, Phys. Rev. **75**, 1969 (1949)
17. O. Haxel, H.H.D. Jensen, H.E. Suess, Phys. Rev. **75**, 1766 (1949)
18. A. Bohr, B. Mottelson, *Nuclear Structure* (Benjamin, New York, 1969)
19. P. Ring, P. Schuck, *The Nuclear Many-Body Problem* (Springer, Berlin, 1980)
20. K. Heyde, *Basic Ideas and Concepts in Nuclear Physics* (Institute of Physics Publishing, Bristol, 1999)
21. J.D. Walecka, Ann. Phys., NY **83**, 491 (1974)
22. B.D. Serot, J.D. Walecka, Adv. Nucl. Phys. **16**, 1 (1986)
23. P.G. Reinhard, Rep. Prog. Phys. **52**, 439 (1989)
24. D. Hirata, H. Toki, T. Watabe, I. Tanihata, B.V. Carlson, Phys. Rev. C **44**, 1467 (1991)
25. P. Ring, Prog. Part. Nucl. Phys. **37**, 193 (1996)
26. M. Brack, C. Guet, B. Hakansson, Phys. Rep. **123**, 275 (1985)
27. A. Sobiczewski, Fiz. Elem. Chastits At. Yadra **295**, 25 (1994)
28. P. Möller, J.R. Nix, W.D. Myers, W.J. Swiatecki, At. Data Nucl. Data Tables **59**, 185 (1995)
29. P. Möller, J.R. Nix, K. Kratz, At. Data Nucl. Tables **66**, 131 (1997)
30. V.Y. Denisov, Phys. At. Nucl. **68**, 1133 (2005)
31. J.F. Berger, L. Bitaud, M. Girod, K. Dietrich, Nucl. Phys. A **685**, 644 (2001)
32. M. Bender, W. Nazarewicz, P.-G. Reinhard, Phys. Lett. B **515**, 42 (2001)
33. M. Bender, K. Rutz, P.-G. Reinhard, J.A. Maruhn, W. Greiner, Phys. Rev. C **60**, 034304 (1999)
34. T. Bürvenich, K. Rutz, M. Bender, P.G. Reinhard, J.A. Maruhn, W. Greiner, Eur. Phys. J. A **3**, 139 (1998)
35. A.T. Kruppa, M. Bender, W. Nazarewicz, P.G. Reinhard, T. Vertse, S. Čwiok, Phys. Rev. C **61**, 034313 (2000)
36. S. Liran, A. Marinov, N. Zeldes, Phys. Rev. C **62**, 047301 (2000)
37. S. Liran, A. Marinov, N. Zeldes, Phys. Rev. C **66**, 024303 (2000)
38. G. Lalazissis, M. Sharma, P. Ring, Y. Gambhir, Nucl. Phys. A **608**, 202 (1996)
39. S. Ćwiok, J.F. Dobaczewski, P. Magierski, W. Heenen, Nazarewicz P. H., Nucl. Phys. A **611**, 211 (1996)
40. K. Rutz, M. Bender, T. Bürvenich, T. Schilling, P.G. Reinhard, J.A. Maruhn, W. Greiner, Rev. C **56**, 238 (1997)
41. T. Bürvenich, K. Rutz, M. Bender, et al., Eur. Phys. J. A **3**, 139 (1998)
42. A.T. Kruppa, M. Bender, W. Nazarewicz, et al., Phys. Rev. C **61**, 034313 (2000)
43. T. Sil, S.K. Patra, B.K. Sharma, M. Centelles, X. Vinas, Phys. Rev. C **69**, 044315 (2004)
44. M. Bhuyan, S.K. Patra, Mod. Phys. Lett. A **27**, 1250173 (2012)
45. W. Zhang, J. Meng, S.Q. Zhang, L.S. Geng, H. Toki, Nucl. Phys. A **753**, 106 (2005)
46. H. Nakada, K. Sugiura, Prog. Theor. Exp. Phys. **2**, 033D02 (2014)
47. H. Nakada, Phys. Rev. C **87**, 014336 (2013)
48. J.F. Berger, M. Girod, D. Gogny, Comput. Phys. Commun. **63**, 365 (1991)
49. S. Goriely, S. Hilaire, M. Girod, S. Përu, Phys. Rev. Lett. **102**, 242501 (2009)
50. M. Ismail, A.Y. Ellithi, A. Adel, H. Anwer, J. Phys. G: Nucl. Part. Phys. **43**, 015101 (2016)
51. M. Ikram, A.A. Rather, S.K. Biswal, B. Kumar, S.K. Patra, Int. J. Mod. Phys. E **25**, 1650103 (2016)
52. Y. Sugahara, H. Toki, Prog. Theor. Phys. **92**, 803 (1994)
53. D. Vretenar, W. Pos̆chl, G.A. Lalazissis, P. Ring, Phys. Rev. C **57**, R1060 (1998)
54. H.-F. Lü, J. Meng, S.Q. Zhang, S.G. Zhou, Eur. Phys. J. A **17**, 19 (2003)
55. M.T. Win, K. Hagino, Phys. Rev. C **78**, 054311 (2008)
56. M. Ikram, S.K. Singh, A.A. Usmani, S.K. Patra, Int. J. Mod. Phys. E **23**, 1450052 (2014)
57. N.K. Glendenning, D. Von-Eiff, M. Haft, H. Lenske, M.K. Weigel, Phys. Rev. C **48**, 889 (1993)
58. J. Mares, B.K. Jennings, Phys. Rev. C **49**, 2472 (1994)
59. M. Rufa, J. Schaffner, J. Maruhn, H. Stöcker, W. Greiner, Phys. Rev. C **42**, 2469 (1990)
60. J. Schaffner, M. Hanauske, H. Stöcker, W. Greiner, Phys. Rev. Lett. **89**, 171101 (2002)
61. H. Shen, F. Yang, H. Toki, Prog. Theor. Phys. **115**, 325 (2006)
62. J. Schaffner, C.B. Dover, A. Gal, C. Greiner, D.J. Millener, H. Stöcker, Ann. Phys. (N.Y.) **235**, 35 (1994)
63. J. Schaffner, C.B. Dover, A. Gal, C. Greiner, H. Stöcker, Phys. Rev. Lett. **71**, 1328 (1993)
64. G.A. Lalazissis, S. Karatzikos, R. Fossion, D. Pena Arteaga, A.V. Afanasjev, P. Ring, Phys. Lett. B **671**, 36 (2009)
65. C.B. Dover, A. Gal, Prog. Part. Nucl. Phys. **12**, 171 (1984)
66. M. Chiapparini, M.E. Bracco, A. Delfino, M. Malheiro, D.P. Menezes, C. Providencia, Nucl. Phys. A **826**, 178 (2009)
67. N.K. Glendenning, S.A. Moszkowski, Phys. Rev. Lett. **67**, 2414 (1991)
68. S.K. Biswal, B. Kumar, S.K. Patra, Int. J. Mod. Phys. E **25**, 1650090 (2016)
69. P.B. Demorest, T. Pennucci, S.M. Ransom, M.S.E. Roberts, J.W.T. Hessels, Nature (London) **467**, 1081 (2010)
70. J. Antoniadis, et al., Science **340**, 6131 (2013)
71. M. Dutra, Phys. Rev. C **90**, 055203 (2014)
72. G.A. Lalazissis, et al., Phys Lett B **671**, 36 (2009)
73. A. Bohr, B.R. Mottelson, D. Pines, Phys. Rev. C **110**, 936 (1958)
74. P.G. Reinhard, E.W. Otten, Nucl. Phys. A **420**, 173 (1984)
75. M. Bender, P.H. Heenen, P.G. Reinhard, Rev. Mod. Phys. **75**, 121 (2003)
76. J. Blocki, M. Flocard, Nucl. Phys. A **273**, 45 (1976)
77. W. Brückner, et al., Phys. Lett. B **79**, 157 (1978)
78. M. May, Phys. Rev. Lett. **47**, 1106 (1981)
79. M. May, et al., Phys. Rev. Lett. **51**, 2085 (1983)
80. S. Ajimura, et al., Phys. Rev. Lett. **86**, 4255 (2001)